On the Distribution of NBTI Time Constants on a Long, Temperature-Accelerated Time Scale

Gregor Pobegen and Tibor Grasser, *Senior Member, IEEE*

***Abstract*— Recent investigations on individual defects contributing to negative bias temperature instability (NBTI) showed that the emission and capture time constants are thermally activated via an Arrhenius law. We apply this finding to conventional micrometer-sized devices where NBTI is the response of up to millions of defects. We rapidly switch the device temperature using an on-chip heating structure in order to accelerate NBTI stress and recovery and acquire experimental data on an up to 18 decades long time scale. On this extended time scale, we find that the distribution of NBTI defect time constants is log-normal with large mean and variance which follows directly from a normal distribution of energy barriers in Arrhenius law. As such, our work clearly identifies the role of temperature for NBTI and suggests a method for accurate life-time estimations.**

***Index Terms*— Accelerated aging, automotive electronics, high-temperature techniques, lifetime estimation, MOSFETs, NBTI, negative bias temperature instability, oxide and interface defects, power MOSFET, semiconductor device reliability.**

I. Introduction

THE negative bias temperature instability (NBTI) has become one of the most critical reliability issues for silicon-based MOSFETs [1]–[4]. After the discovery of instability, the time dynamics of NBTI degradation has been found to follow roughly a power law [5], which implies the need to analyze experimental data with respect to the logarithm of time. To investigate the physical mechanisms leading to NBTI, extensive experimental datasets over several decades in time are needed. The extension of the experimental time range toward shorter times is laborious but is improved using operational amplifiers [6], which allow to measure transitions with $\approx 1\mu$s resolution. The other limit of the experimental time range is given by the duration of the experiment and does therefore usually not exceed a few weeks ($\approx 10^6$s). We present temperature switches as a means to extend this rather fixed experimental time frame both toward shorter and longer times.

Manuscript received December 6, 2012; revised May 3, 2013; accepted May 3, 2013. Date of current version June 17, 2013. This work was supported in part by the Austrian Research Promotion Agency FFG under Project 831163 and the Carinthian Economic Promotion Fund under Contract KWF-1521/22741/34186. The review of this paper was arranged by Editor H. Jaouen.

G. Pobegen is with Kompetenzzentrum für Automobil- und Industrieelektronik GmbH, Villach 9500, Austria, and also with the Institute for Microelectronics, Vienna University of Technology, Vienna 1040, Austria (e-mail: gregor.pobegen@k-ai.at).

T. Grasser is with the Institute for Microelectronics, Vienna University of Technology, Vienna 1040, Austria (e-mail: grasser@iue.tuwien.ac.at).

Color versions of one or more of the figures in this paper are available online at http://ieeexplore.ieee.org.

Digital Object Identifier 10.1109/TED.2013.2264816

We base our method on the recently identified Arrhenius activation of individual defect time constants [7], [8] and apply it to micrometer-sized devices with a large number of defects with distributed time constants. To handle an arbitrary distribution of time constants, we construct an abstract temperature–time which gives us the possibility to transform experimental data to other time frames. We perform our experiments using the recently developed poly-heater [9] in order to quickly ($< 1s$) switch the device temperature. The poly-heater allows for device temperature switches on wafer level through controlling the power dissipated in two polysilicon wires situated in close vicinity of the device under test.

After giving insight into the analysis of our data at different temperatures, we describe the details of our experiments. We then show separately for NBTI recovery and degradation that the Arrhenius-like temperature activation allows for reliable extensions of the experimentally accessible time frame. We then maximize the acceleration using very high stress temperatures to assess the long-term behavior of NBTI degradation. We show that the degradation behavior on this extended measurement range is consistent with a normal distribution of the effective activation energies of the NBTI defects. The normal distribution is observed with different parameters for various different MOSFETs, with both standard SiO_2 or SiON dielectrics.

II. Background

NBTI is commonly considered to occur at or near the dielectric–semiconductor interface as the creation of new crystallographic defects or the charging of existing defect precursors [1], [2]. Both of these processes have in common that one or more atomic bonds are broken followed by a structural transformation of the vicinity. The structural transformation may be the motion of a hydrogen atom [1] away from the defect site after the depassivation of a Si dangling bond at the interface (P_b center) or the transition of a charged precursor into a puckered configuration [2]. Possible candidates for the latter defect type are the E' center [10], the K_N center [11] or the hydrogen bridge [12]. The energy needed for the breakage of an atomic bond depends heavily on the vibrational properties of the bond. Consequently, the effective energy needed to break the bond requires several individual phonons [13], [14]. This multiphonon contribution leads to a temperature activation of the capture cross sections, which in the classical limit obeys an Arrhenius law [15]. The defect time constants are proportional to the inverse of the capture cross-section and therefore have the same temperature

0018-9383/$31.00 © 2013 IEEE

activation

$$\tau = \tau_0 \exp\left(\frac{E_B}{k_B T}\right) \quad (1)$$

with an energy barrier E_B and Boltzmann's constant k_B. Just as the effective activation energy E_B, τ_0 will be different for every single defect [8] and, in particular, depend on the depth x of the defect in the oxide. However, given the experimental evidence that shows no correlation between τ_0 and x [16], we assume τ_0 to be the same for all defects [17]. Naturally, (1) is way too simple to cover the rich features of individual defects [2]. Still, as will be shown, it reasonably well captures the temperature dependence of defects at fixed bias, especially the behavior of a large ensemble of individual defects. In particular, τ_0 is considered an effective average value and the only fit parameter of our extraction scheme.

Assuming the energy barrier to be temperature independent, we can deduce how a defect time constant changes from τ_1 to τ_2 when changing the temperature from T_1 to T_2. This can be seen by solving (1) for E_B

$$E_B = k_B T \ln \frac{\tau}{\tau_0} \quad (2)$$

and calculating

$$\tau_2 = \tau_0 \exp\left(\frac{k_B T_1 \ln(\tau_1/\tau_0)}{k_B T_2}\right) = \tau_0 \left(\frac{\tau_1}{\tau_0}\right)^{T_1/T_2}. \quad (3)$$

This equation allows for the definition of the *temperature–time* ϑ as [18]

$$\vartheta(T) = \tau_0 \left(\frac{t}{\tau_0}\right)^{T_{meas}/T} \quad (4)$$

which is used to transform experimental data measured at the temperature T_{meas} to any other reference temperature T. Providing the physical correctness of our assumption, this approach makes it possible to transform data from a fixed experimental window (say 10^{-6}s to 10^{6}s) to an extended time frame. For example, measuring at colder temperatures than the reference temperature rescales the time axis toward smaller values. This allows decelerating fast transitions to measure them with reasonable measurement intervals on conventional equipment. Such fast transitions occur especially right after the end of a negative bias stress phase and have been shown to introduce significant errors in lifetime extrapolations [6], [19]. On the other hand, if $T_{meas} > T$, defects with time constants much larger than what can be reasonably observed otherwise may be analyzed in a short-time experiment. This considerably extends the experimentally accessible time scales.

All considerations that follow are based on the assumption that NBTI is the response of a large number of defects which behave approximately as a first-order process with the time constants given by (1). The applicability of this assumption has been demonstrated previously [4], [17], [18], [20]. We remark that the assumption that (1) is valid does not imply that we assume that NBTI is due to a single component and whether charge trapping or interface state creation are dominant [1], [4], [11], [19], [20], as long as these processes follow roughly a first-order process as indicated by our previous results [17]. In contrast to previous studies, which were limited to conventional experimental windows, we identify the underlying distribution for NBTI defect time constants on significantly extended time scales. We find that the time constants are distributed following a log-normal distribution which is due to an underlying normal distribution of effective energy barriers. The distribution of energy barriers is due to the distribution of the dissociation energies of the atoms which compose the defect site. The assumption of normally distributed dissociation energies is consistent with previous work for the silicon–hydrogen bond at the Si–SiO_2 interface [4], [17], [21] as well as for oxide defects [17].

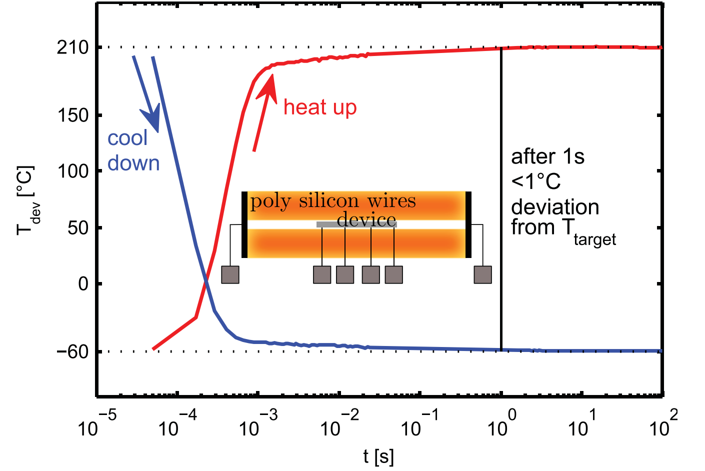

Fig. 1. Heating and cooling characteristics of a device surrounded by a poly-heater (the layout sketch in the inset). When switching the power supplied to the poly-heater abruptly on or off, the device temperature follows with ∼ 1 ms delay because of the thermal capacitance of the surrounding materials. The difference in the desired target temperature becomes smaller than 1 °C after roughly a second.

III. Experimental

Performing NBTI measurements at different temperatures using a thermo chuck is a time-consuming activity. On conventional systems, temperature switches of only 100 °C usually take already several minutes and a lot of experimental efforts are required to avoid losing needle contact because of thermal expansion. Furthermore, it becomes increasingly complicated to build thermo chuck systems that are able to handle more than 300 °C [22]. All those issues may be easily overcome when using the poly-heater, a simple local heating structure surrounding the device, originally developed for fast wafer level reliability characterization [23].

A. Use of the Poly-heater

We elevate the temperature of the device under test through joule heating of two closely located polycrystalline silicon wires. A sketch of the poly-heater is given in the inset of Fig. 1.

To determine the device temperature T_{dev} while supplying power to the poly-heater, we use the dependence of the drain current I_D on temperature. The measurement of T_{dev} using the drain current directly links to the temperature of Si–SiO_2 interface. Finite element method calculations of the temperature

gradients within the device/poly-heater stack revealed that the gradients within the device are less than 1 °C, even for a large temperature difference of ≈ 225 °C between the device and the chuck [23]. Determining the device temperature directly at the Si–SiO_2 interface is highly beneficial for NBTI testing because the degradation is commonly assumed to occur at the interface or in close vicinity to it.

In detail, we record the dependence of I_D on the temperature using the thermo chuck prior to stress at a suitably chosen operating point. This gives us a relation $I_D(T)$ which allows to transform any change in I_D due to changes in the poly-heater supply power to changes of the device temperature [9]. Unfortunately, this procedure has the drawback that it can only be applied within the temperature range of the thermo chuck. But even with the availability of thermo chuck systems for temperature >300 °C, an extrapolation procedure is needed to determine T_{dev} because silicon starts to become intrinsic at these high temperatures and I_D fails to reflect the device temperature. We therefore extrapolate the dependence of T_{dev} on the poly-heater power supply taking the change of the thermal resistance of silicon with temperature into account. We later use this extrapolation to map the power dissipated in the heater to the device temperature [24]. This approach is shown to have a relative error smaller than 5% up to a 260 °C temperature switch [18], [24].

B. Samples

We begin by elaborating the temperature dependence of defect charging/discharging on SiO_2 and SiON-based devices. The SiO_2 samples are large area 100 × 6 μm devices and have a 30 nm thick oxide as required for power applications. The SiON samples are 10 × 0.12 μm gate area devices with a 2.2 nm plasma nitrided oxide [6].

The ΔV_{TH} is measured by mapping changes in the drain current at a gate voltage close to the V_{TH} to a corresponding drift using a transfer characteristic of the virgin device [25].

IV. Temperature Dependence of NBTI Recovery

In Fig. 2, the NBTI recovery temperature dependence is investigated independently of the stress temperature.

Following several stresses with always the same temperature (100 °C), oxide field and duration, we analyzed the NBTI recovery at temperatures between −60 °C and 250 °C for 100 s. To avoid inaccuracies related to device-to-device variability, the measurements are performed consecutively on a single device with intermediate bake steps (10 s at 300 °C) at zero gate bias to recover from all previous damage of the device [18], [26], [27]. When returning to the virgin state of the device with this sufficiently long bake phase, we do not observe the interesting phenomenon of defect loss as described in other recent work [28]. This is consistent with our previous results obtained in a similar technology, where defect loss is observed to be marginal [17]. We switch the temperature from T_{str} to T_{chuck} 10 s before the interruption of the stress gate bias in order to maintain the degradation level (degradation quenching [29]). The end of the stress is then defined by the switch of the gate bias from stress to recovery level. We

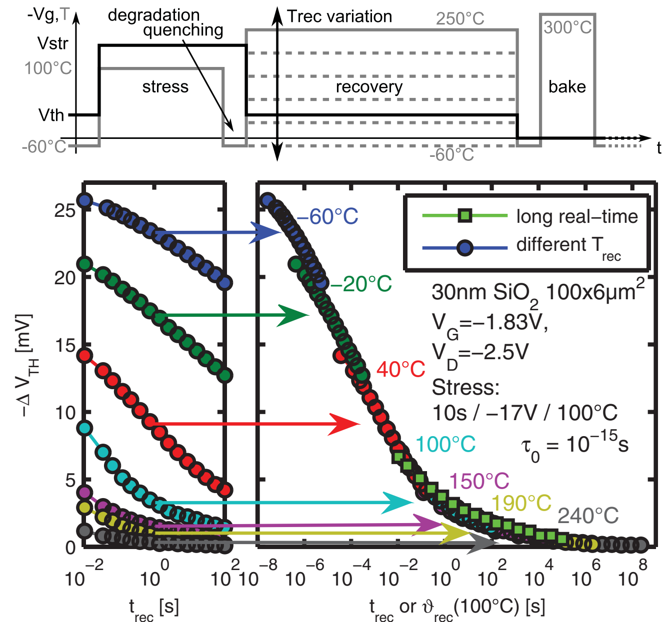

Fig. 2. The poly-heater allows to measure recovery at different temperatures following a stress sequence at always the same temperature (here 100 °C). When the recovery traces are plotted as a function of time since end of stress (left), one observes that the measured degradation is larger at lower temperatures. This result may be understood when the data is interpreted with the temperature–time (4) (right). With a suitably chosen τ_0, all recovery transients match to a single universal trace and reproduce a long real-time measurement at 100 °C chuck temperature (square symbols). The real-time duration of the temperature accelerated measurement is approximately 1 h.

interpret the subsequently recorded recovery data in terms of the temperature–time (4) and determine an average τ_0 for all defects by minimizing the vertical difference in the overlapping data of Fig. 2. We observe one single universal recovery trace which reproduces a two day long reference measurement at 100 °C chuck temperature. We note that the quality of the fit can be improved by considering two independent distributions with different values for τ_0 as done previously [17]. However, we consider a single effective distribution with a single τ_0 to be sufficiently accurate for our present purposes. This result confirms that the temperature dependence of NBTI recovery can be understood by a simple collection of temperature-activated first-order processes: At low temperatures, the time constants become larger and thus only a small number of defects are able to anneal. Consequently, the number of remaining charges and thus the measured ΔV_{TH} is large. With increasing temperature, the time constants become shorter and most of the charges leave the defect during the recovery measurement. In the extreme case, when the recovery temperature even exceeds the stress temperature, nearly all of the defects which have been created during stress anneal already before the first measurement point after a 10 ms real-time delay, resulting in a very small ΔV_{TH}.

The recovery trace at different temperatures may also be obtained in a single measurement through temperature switches during recovery, as depicted in Fig. 3.

Care has to be taken that temperature switches create spurious V_{TH} shifts during the period of unstable temperature, which have to be considered in order to acquire the result

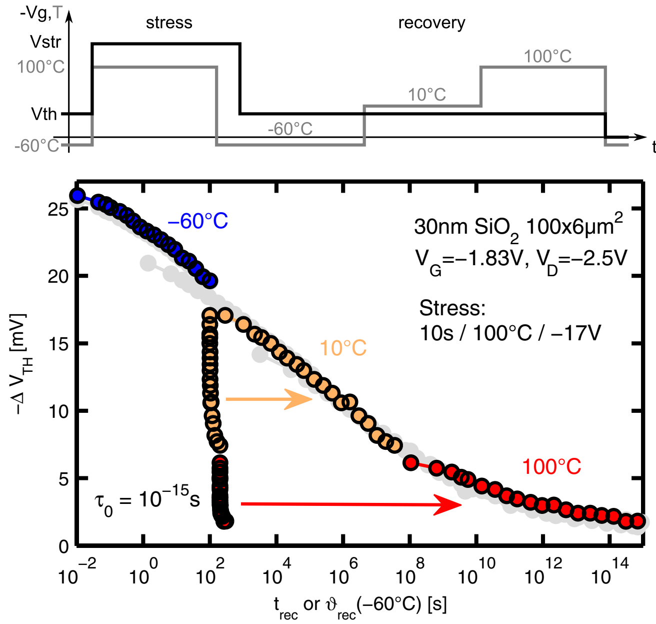

Fig. 3. Universal recovery trace of Fig. 2 obtained with several independent measurements (gray symbols). The same transient may also be gathered when performing temperature switches during the recovery (colored symbols). The effect of the higher temperature is an apparent shift to the right along the time axis.

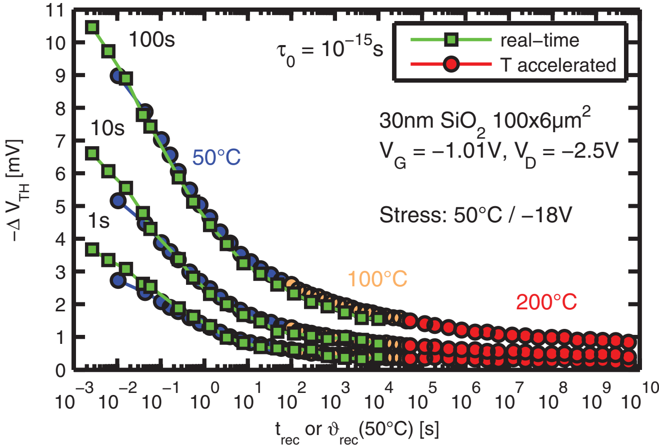

Fig. 4. Increasing the temperature during recovery can be used to access the long-term recovery transients after moderate NBT stress. The temperature accelerated data reproduces the real-time measurement in a convincing way and extends the traces considerably. The experimental time window of 10^4s $\approx$ 3 h is straightforwardly lengthened to otherwise infeasibly long durations 10^{10} s $\approx$ 300 years).

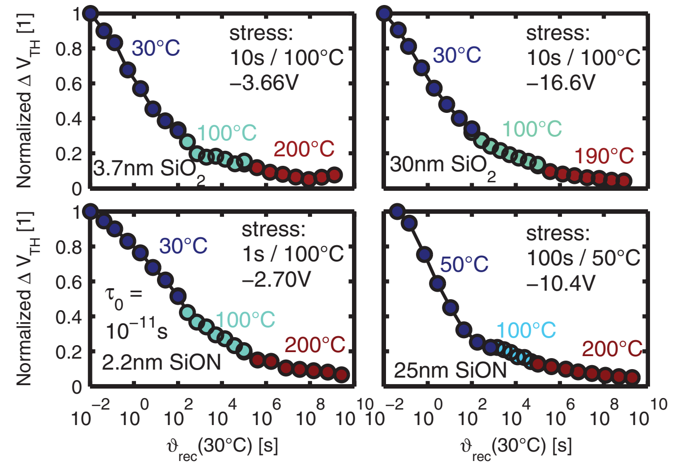

Fig. 5. Experiment of Fig. 4 repeated on several different MOSFET technologies. The temperature–time concept (4) is applicable independently of the type of oxide with a single guess of $\tau_0 = 10^{-11}$s. All investigated technologies show roughly the same distribution of NBTI recovery time constants. The remaining fraction of degradation after long recovery times happens to be very small on all investigated technologies.

shown. Details concerning this effect are described in [30]. The effect of the time transformation (4) is to shift the experimental data along the time axis to much larger values. This allows extending the recovery transients to otherwise impractically long times, as depicted in Fig. 4.

In particular, the approach allows for the analysis of defects with very large time constants, usually labeled as permanent or quasi-permanent degradation [4], [31]. We remark that further acceleration of the recovery with higher temperatures can lead to degradation even at V_{TH}, especially in devices with thin gate oxides, which can lead to the appearance of erroneous plateaus in the recovery transient [31]. For this reason, recovery acceleration appears mostly beneficial for moderate stress conditions where the stress temperature is considerably lower than the maximum allowed recovery temperature. An investigation of the quasi-permanent component by temperature acceleration of the recovery following moderate NBT stress depicted in Fig. 5 shows that the remaining level of degradation is rather small in devices with SiO_2 or SiON technology. Furthermore, the concept of temperature acceleration for recovery appears to work in a wide variety of technologies with similar values of τ_0.

This justifies the use of temperature switches during recovery for the measurement of NBTI recovery data to acquire experimental datasets on long time scales.

V. Temperature Dependence of NBTI Degradation

In order to investigate the NBT stress temperature dependence we use measurement-stress-measurement (MSM) experiments where the NBTI stress is interrupted through short switches to V_{TH} to monitor the degradation. Here, the polyheater allows to stress at arbitrary temperatures T_{str} while the degradation may be monitored at always the same, substantially lower chuck temperature T_{chuck}. The interruption of the stress can be performed at low temperatures which keeps unwanted recovery small. When we account for the different recovery delay times at different chuck temperatures by using the temperature-time (4) we are able to compare T accelerated MSM data to real-time data, as depicted in Fig. 6. The T accelerated data is in agreement with the real-time data and exhibits in particular the same gradual change in the power law exponent as the real-time data. The T acceleration appears therefore to be applicable to extend the experimental accessible time range to acquire large experimental stress datasets in a short amount of time.

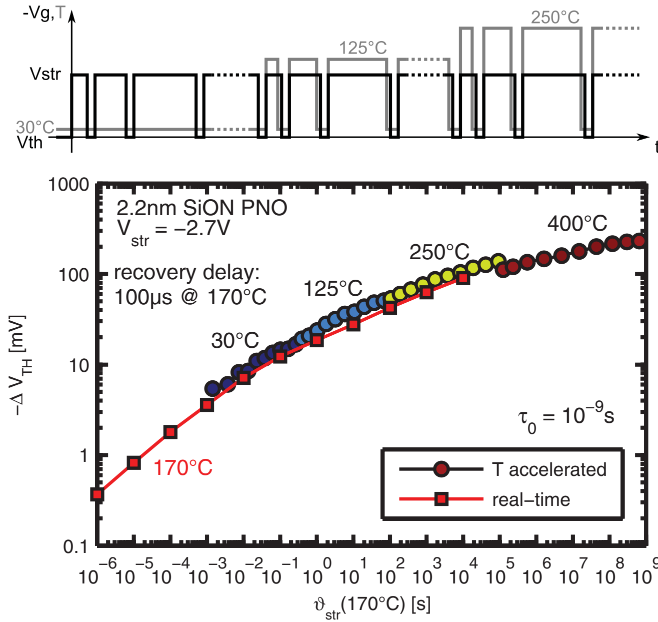

Fig. 6. Comparison of a half week long real-time MSM experiment from [17] (performed on a different wafer of the same technology with a different measurement equipment) with a temperature accelerated MSM experiment of approximately one-hour duration. The real-time MSM experiment measured the degradation with a 100 μs delay, which decreases the ΔV_{TH} value due to recovery. These 100 μs at 170 °C correspond to approximately 20 ms at 30 °C for the temperature accelerated measurement.

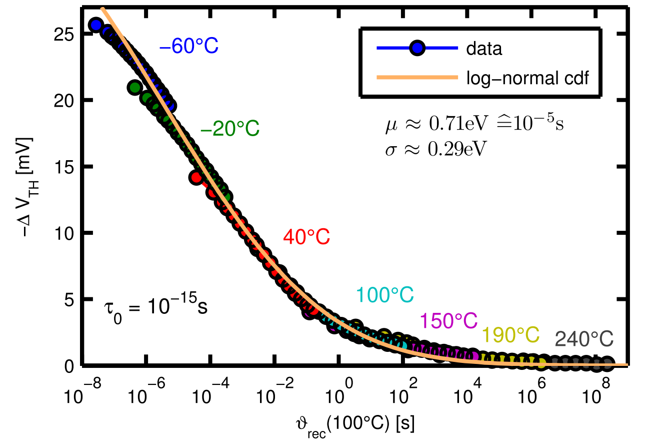

Fig. 7. Data of Fig. 2 spans over a range of 16 decades in time. We use this large data set to test our assumption that the distribution of emission time constants is a log-normal cumulative distribution function after (5) with large σ.

VI. Results and Discussion

In the preceding paragraphs, we showed that the interpretation of NBTI degradation and recovery data at different temperatures with the temperature–time (4) gives results consistent with real-time data. This gives us the possibility to analyze NBTI degradation on a very long time scale.

A. Recovery Behavior

NBTI recovery is assumed to be the sum of a large number of single discharging events with distributed emission time constants [20], [32]. Because of (2), the distribution of time constants can be mapped onto a distribution of effective emission barrier energies. When we assume the energy barriers to be normally distributed, it follows that recovery has to obey [17]

$$\Delta V_{\mathrm{TH}}^{\mathrm{rec}} = \frac{\Delta V_{\mathrm{TH}}^{\mathrm{max}}}{2}\,\mathrm{erfc}\left(\frac{k_{\mathrm{B}}T\,\ln\frac{\vartheta_{\mathrm{rec}}}{\tau_0}-\mu}{\sqrt{2}\sigma}\right) \tag{5}$$

where $\Delta \mathrm{V}_{\mathrm{TH}}^{\mathrm{max}}$ is the maximum drift after the given stress, μ, σ are the parameters of the normal distribution of the energy barriers and erfc is the complementary error function. When we fit the parameters of the distribution to our experimental recovery data, as depicted in Fig. 7, we observe a good agreement over the very large range of ∼16 decades in time.

B. Degradation Saturation

To acquire a large data set for NBTI degradation, we perform MSM experiments on four equivalent devices with stress temperatures up to 400 °C, see Fig. 8. We observe a slow but continuous decrease of the power law coefficient. Although it is mandatory for the degradation to saturate from a microscopic perspective, as eventually all possible defect sites have become created at a certain time, the details on how the power law coefficient decreases is a very interesting observation which is mentioned only rarely [4], [33]. This is primarily due to the logarithmic nature of NBTI degradation and the consequential extreme need of measurement time. We compare the saturation behavior with the prediction of reaction–diffusion (RD) theory [1], [3] and the assumption of normally distributed energy barriers which leads to a distribution of NBTI defect capture time constants following a cumulative log-normal distribution function as

$$\Delta \mathrm{V}_{\mathrm{TH}}^{\mathrm{str}} = \frac{\Delta \mathrm{V}_{\mathrm{TH}}^{\mathrm{max}}}{2}\,\mathrm{erfc}\left(-\frac{k_{\mathrm{B}}T\,\ln\frac{\vartheta_{\mathrm{str}}}{\tau_0}-\mu}{\sqrt{2}\sigma}\right). \tag{6}$$

$\Delta \mathrm{V}_{\mathrm{TH}}^{\mathrm{max}}$ is, in this case, the maximum drift capability of the device for a given stress oxide field.

We observe that the degradation behavior can be perfectly explained over 18 decades in time with the assumption of normally distributed energy barriers E_{B}. Due to (2), the derivative of $\Delta V_{\mathrm{TH}}(\lg \vartheta_{\mathrm{str}})$ directly gives the distribution of the time constants with respect to their capture time or capture energy barrier. The change of the power law coefficient can be calculated when differentiating $\lg \Delta V_{\mathrm{TH}}(\lg \vartheta_{\mathrm{str}})$ and is depicted in the bottom plot of Fig. 8. The slow decrease of the power law coefficient n is a consequence of the derivative of the logarithm of the erfc in (6). We remark that the decrease of n occurs continuously at all temperature and time and remains invisible when analyzing only a small fraction of the degradation behavior in typical real-time experiments.

The decrease of the power law coefficient with higher T interpreted with the temperature–time is in contrast to some previous studies [4], which suggested that n increases linearly with temperature. This finding is related to the equivalent stress and recovery temperature used in conventional experiments. While the power law coefficient changes only slightly

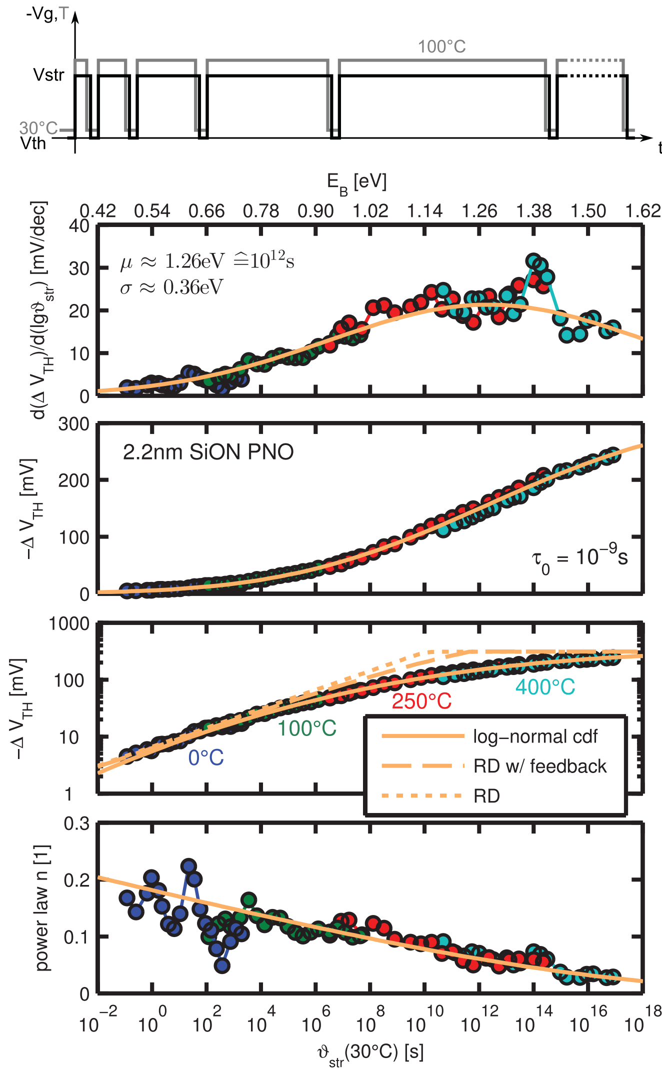

Fig. 8. Temperature accelerated MSM experiment on four different 2.2 nm SiON pMOS devices with stress temperatures up to 400 °C over 18 decades in time. The initial data up to roughly the maximum feasible real-time stress duration exhibits a power law coefficient of $n \approx 1/6$ (RD). At large times or high temperatures, the degradation dynamic clearly saturates. The saturation behavior is at odds with the prediction of standard RD theory, which states that at a certain point in time all hydrogen is released from the Si–SiO_2 interface and the degradation stops rather abruptly [3]. Also, consideration of the decrease of the stress oxide field due to the reduction of $V_{str} - V_{TH}$ with increasing ΔV_{TH} cannot totally account for the observed power law saturation (RD with feedback). The data (symbols) are compared to a fitted log-normal distribution of the capture time constants for the NBTI defects (log-normal cdf) on four different axes as described in the text. Capture times and capture energy barriers are linked via (1) for a fixed τ_0.

with stress temperature [1], [3], n increases with measurement delay after the end of stress due to recovery [6], [19]. As higher temperatures are equivalent to longer delay (cf. Fig. 2) the increase of n with T in experiments with equal stress and recovery temperatures is due to the increase of n with measurement delay.

C. Stress Bias Influence

Our acceleration approach allows us to investigate the saturation behavior for different stress gate biases, as depicted in Fig. 9.

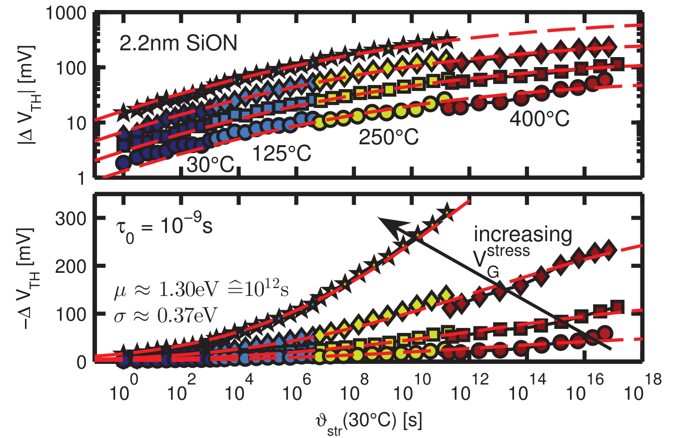

Fig. 9. Acceleration with increasing stress temperatures for different stress voltages. The saturation occurs roughly at always the same time, which suggests that only the number of available defects changes with stress voltage. The real-time duration of all four measurements on four different devices was approximately 4 h.

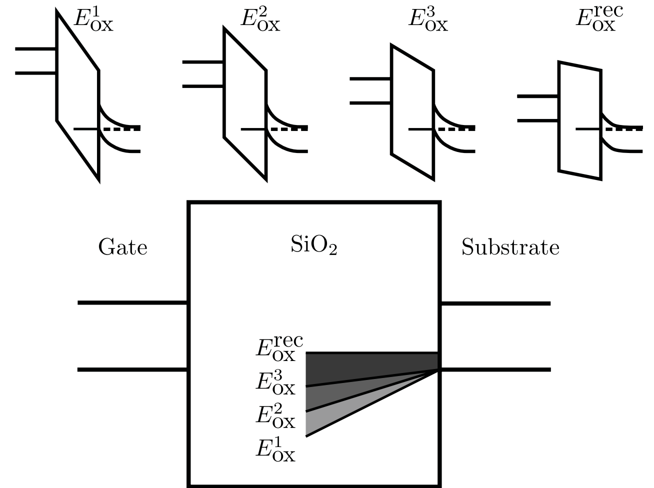

Fig. 10. The gate bias during stress and recovery changes the active energy region for the defects, which can possibly contribute to the drift of the device. With increasing stress bias (and thus increasing stress oxide field E_{ox}), the active energy region increases gradually.

We observe that the stress oxide field leaves the parameters μ and σ of the distribution mostly unaffected (only a minor decrease of μ and σ with V_{str} is observed). The stress voltage mainly influences the number of activated defects ΔV_{TH}^{max}. This is emphasized in Fig. 9 with the fit of a single log-normal cumulative distribution function with single values of μ and σ, but different amplitudes ΔV_{TH}^{max} for the different stress voltages. The increase of the number of charges with increasing stress bias is due to the relatively large effect of the increase of the active energy region for traps within the oxide, as sketched in Fig. 10.

The estimation of ΔV_{TH}^{max} allows to investigate the overall number of defect precursor within the device accessible for a given oxide field. When ΔV_{TH}^{max} is converted to a defect density, a value of approximately $10^{12} cm^{-2}$ is obtained, which indicates that NBTI activates only pre-existing defect precursors and does not create a significant number of new defects.

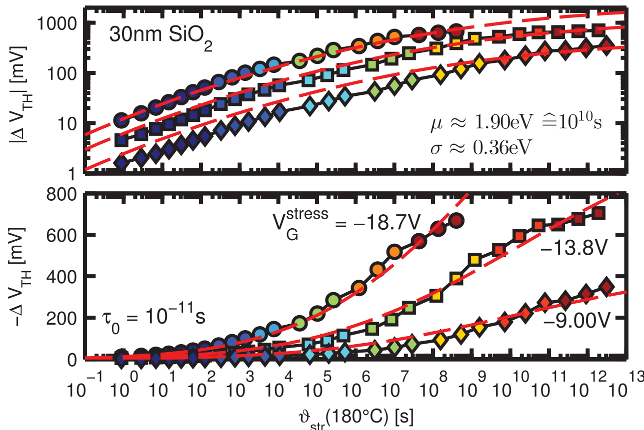

Fig. 11. Gradual change of the power law exponent for 30 nm SiO_2 technology devices is similar to that of 2.2 nm technology devices shown in Fig. 9.

The field dependence of the maximum degradation in Fig. 9 is $\propto E_{ox}^{3.3}$ which is around the commonly measured value for the oxide field dependence [20], [34].

We remark that the relatively large ΔV_{TH} values in our saturation experiment may decrease the effective stress gate bias V_G^{stress} and could therefore in principle contribute to a saturation. However, this feedback has only a small impact on the saturation because of the following observations. The power law coefficient decreases simultaneously for all tested oxide field values and does not occur earlier for low oxide fields, where the relative influence of ΔV_{TH} on V_G^{stress} is large. This means in particular that the saturation is independent of the absolute ΔV_{TH} value and thus independent of the rather small decrease of the oxide field. Consider also Fig. 8, where we calculated the saturation dynamics of this feedback effect for particular example data. Furthermore, we have observed an equivalent saturation behavior on thick oxide (30 nm) devices, as depicted in Fig. 11, where the ΔV_{TH} is very small compared to V_G^{stress}.

D. Sensitivity to τ_0

The basic effect of τ_0 is to shift the experimental data slightly along the temperature–time axis. The values used in this paper are justified by their ability to scale the data to form continuous transients. However, these values must be considered effective values of the actual distribution of τ_0, which might be different in different technologies.

The fact that τ_0 is also distributed is apparent from time-dependent-defect-spectroscopy measurements where a handful of individual defects have very different values of τ_0 [7], [8]. The mean value of τ_0 for a large number of defects may be found when analyzing an increasing number of devices of a single technology and deducing a mean τ_0 through fitting an analytical model to the degradation data, as suggested in [17]. Even if this procedure introduces an error, the sensitivity of the extrapolation to τ_0 is small.

VII. Conclusion

We studied the influence of the temperature on NBTI in SiON or SiO_2-based pMOSFETs using temperature switches during the application of gate bias. This became feasible when using the poly-heater, an on-chip local heating structure. By introducing an abstract temperature–time (4), which followed directly from a simple Arrhenius equation, we plotted measurement data recorded at different temperatures in a more intuitive way. This concept allowed for acceleration or deceleration of stress and recovery processes, making it possible to obtain measurement data on time scales much longer than what is feasible in a real-time experiment. On these large datasets, we observed that the degradation and recovery was due to log-normally distributed capture and emission time constants with large mean and variance. We suggested that this distribution was a consequence of normally distributed energy barriers E_B for inelastic charging processes of defect precursors or the reaction limited breakage of silicon–hydrogen bonds at the interface.

Furthermore, our findings can be utilized for the acceleration through temperature to considerably reduce the time effort and uncertainty when performing NBTI tests for device reliability estimation.

Acknowledgment

The authors would like to thank M. Nelhiebel and T. Aichinger (both Infineon Technologies Austria AG) for various inspiring discussions and K.-H. Gebhardt, M. Müller, H. Reisinger, and R. Vollertsen (all Infineon Technologies AG, Germany) for their kind support.

References

[1] S. Mahapatra, A. E. Islam, S. Deora, V. D. Maheta, K. Joshi, A. Jain, and M. A. Alam, “A critical re-evaluation of the usefulness of R-D framework in predicting NBTI stress and recovery,” in *Proc. IEEE Int. Rel. Phys. Symp.*, Apr. 2011, pp. 614–623.

[2] T. Grasser, “Stochastic charge trapping in oxides: From random telegraph noise to bias temperature instabilities,” *Microelectron. Rel.*, vol. 52, no. 1, pp. 39–70, 2012.

[3] M. A. Alam and S. Mahapatra, “A comprehensive model of pMOS NBTI degradation,” *Microelectron. Rel.*, vol. 45, no. 1, pp. 71–81, 2005.

[4] V. Huard, M. Denais, and C. Parthasarathy, “NBTI degradation: From physical mechanisms to modelling,” *Microelectron. Rel.*, vol. 46, no. 1, pp. 1–23, 2006.

[5] K. O. Jeppson and C. M. Svensson, “Negative bias stress of MOS devices at high electric fields and degradation of MNOS devices,” *J. Appl. Phys.*, vol. 48, no. 5, pp. 2004–2014, 1977.

[6] H. Reisinger, O. Blank, W. Heinrigs, A. Muhlhoff, W. Gustin, and C. Schlunder, “Analysis of NBTI degradation- and recovery-behavior based on ultra fast Vt-measurements,” in *Proc. IEEE Int. Rel. Phys. Symp.*, Mar. 2006, pp. 448–453.

[7] T. Grasser, H. Reisinger, P. Wagner, F. Schanovsky, W. Goes, and B. Kaczer, “The time dependent defect spectroscopy (TDDS) for the characterization of the bias temperature instability,” in *Proc. IEEE Int. Rel. Phys. Symp.*, May 2010, pp. 16–25.

[8] M. Toledano-Luque, B. Kaczer, P. Roussel, M. J. Cho, T. Grasser, and G. Groeseneken, “Temperature dependence of the emission and capture times of SiON individual traps after positive bias temperature stress,” *J. Vacuum Sci. Technol. B*, vol. 29, no. 1, pp. 01AA04-1–01AA04-5, 2011.

[9] T. Aichinger, M. Nelhiebel, S. Einspieler, and T. Grasser, “In situ poly-heater–A reliable tool for performing fast and defined temperature switches on chip,” *IEEE Trans. Device Mater. Rel.*, vol. 10, no. 1, pp. 3–8, Mar. 2010.

[10] J. Ryan, P. Lenahan, T. Grasser, and H. Enichlmair, “Recovery-free electron spin resonance observations of NBTI degradation,” in *Proc. IEEE Int. Rel. Phys. Symp.*, May 2010, pp. 43–49.

[11] J. Campbell, P. Lenahan, A. Krishnan, and S. Krishnan, "Atomic-scale defects involved in NBTI in plasma-nitrided pMOSFETs," in *Proc. IEEE Int. Integr. Rel. Workshop*, Oct. 2007, pp. 12–17.

[12] P. E. Bloechl and J. H. Stathis, "Aspects of defects in silica related to dielectric breakdown of gate oxides in MOSFETs," *Phys. B, Condensed Matter*, vols. 273–274, pp. 1022–1026, Dec. 1999.

[13] V. Karpus and V. Perel, "Multiphoton ionization of deep centers in semiconductors in an electric field," *J. Experim. Theoretical Phys.*, vol. 64, no. 6, pp. 1376–1383, Dec. 1986.

[14] S. D. Ganichev, E. Ziemann, W. Prettl, I. N. Yassievich, A. A. Istratov, and E. R. Weber, "Distinction between the Poole-Frenkel and tunneling models of electric-field-stimulated carrier emission from deep levels in semiconductors," *Phys. Rev. B*, vol. 61, no. 15, pp. 10361–10365, Apr. 2000.

[15] M. J. Kirton and M. J. Uren, "Noise in solid-state microstructures: A new perspective on individual defects, interface states and low-frequency (1/f) noise," *Adv. Phys.*, vol. 38, no. 4, pp. 367–468, 1989.

[16] T. Nagumo, K. Takeuchi, T. Hase, and Y. Hayashi, "Statistical characterization of trap position, energy, amplitude and time constants by RTN measurement of multiple individual traps," in *Proc. IEEE IEDM*, Dec. 2010, pp. 28.3.1–28.3.4.

[17] T. Grasser, P. Wagner, H. Reisinger, T. Aichinger, G. Pobegen, M. Nelhiebel, and B. Kaczer, "Analytic modeling of the bias temperature instability using capture/emission time maps," in *Proc. IEEE IEDM*, Dec. 2011, pp. 27.4.1–27.4.4.

[18] G. Pobegen, T. Aichinger, M. Nelhiebel, and T. Grasser, "Understanding temperature acceleration for NBTI," in *Proc. IEEE IEDM*, Dec. 2011, pp. 27.3.1–27.3.4.

[19] A. Islam, H. Kufluoglu, D. Varghese, S. Mahapatra, and M. Alam, "Recent issues in negative-bias temperature instability: Initial degradation, field dependence of interface trap generation, hole trapping effects, and relaxation," *IEEE Trans. Electron Devices*, vol. 54, no. 9, pp. 2143–2154, Sep. 2007.

[20] V. Huard, "Two independent components modeling for negative bias temperature instability," in *Proc. IEEE Int. Rel. Phys. Symp.*, May 2010, pp. 33–42.

[21] A. Stesmans, "Dissociation kinetics of hydrogen-passivated Pb defects at the (111) Si-SiO_2 interface," *Phys. Rev. B*, vol. 61, no. 12, pp. 8393–8403, Mar. 2000.

[22] P. Borthen and G. Wachutka, "Testing semiconductor devices at extremely highg operating temperatures," *Microelectron. Rel.*, vol. 48, nos. 8–9, pp. 1440–1443, 2008.

[23] W. Muth and W. Walter, "Bias temperature instability assessment of n- and p-channel MOS transistors using a polysilicon resistive heated scribe lane test structure," *Microelectron. Rel.*, vol. 44, no. 8, pp. 1251–1262, 2004.

[24] G. Pobegen, M. Nelhiebel, S. de Filippis, and T. Grasser, "Accurate high temperature measurements using local polysilicon heater structures," *IEEE Trans. Device Mater. Rel.*, doi:10.1109/TDMR.2013.2265015

[25] B. Kaczer, T. Grasser, P. Roussel, J. Martin-Martinez, R. O'Connor, B. O'Sullivan, and G. Groeseneken, "Ubiquitous relaxation in BTI stressing – New evaluation and insights," in *Proc. IEEE Int. Rel. Phys. Symp.*, Mar. 2008, pp. 20–27.

[26] A. A. Katsetos, "Negative bias temperature instability (NBTI) recovery with bake," *Microelectron. Rel.*, vol. 48, pp. 1655–1659, Oct. 2008.

[27] C. Benard, J.-L. Ogier, and D. Goguenheim, "Total recovery of defects generated by negative bias temperature instability (NBTI)," in *Proc. IEEE Int. Integr. Rel. Workshop*, Oct. 2008, pp. 7–11.

[28] M. Duan, J. F. Zhang, Z. Ji, W. D. Zhang, B. Kaczer, S. De Gendt, and G. Groeseneken, "New insights into defect loss, slowdown and device lifetime enhancement," *IEEE Trans. Electron Devices*, vol. 60, no. 1, pp. 413–419, Jan. 2013.

[29] T. Aichinger, M. Nelhiebel, and T. Grasser, "On the temperature dependence of NBTI recovery," *Microelectron. Rel.*, vol. 48, pp. 1178–1184, Nov. 2008.

[30] T. Aichinger, M. Nelhiebel, and T. Grasser, "Unambiguous identification of the NBTI recovery mechanism using ultra-fast temperature changes," in *Proc. IEEE Int. Rel. Phys. Symp.*, Apr. 2009, pp. 2–7.

[31] T. Grasser, T. Aichinger, G. Pobegen, H. Reisinger, P.-J. Wagner, J. Franco, M. Nelhiebel, C. Ortolland, and B. Kaczer, "The 'permanent' component of NBTI: Composition and annealing," in *Proc. IEEE Int. Rel. Phys. Symp.*, Jun. 2011, pp. 605–613.

[32] B. Kaczer, T. Grasser, J. Martin-Martinez, E. Simoen, M. Aoulaiche, P. Roussel, and G. Groeseneken, "NBTI from the perspective of defect states with widely distributed time scales," in *Proc. IEEE Int. Rel. Phys. Symp.*, Apr. 2009, pp. 55–60.

[33] S. Rangan, N. Mielke, and E. Yeh, "Universal recovery behavior of negative bias temperature instability," in *Proc. IEEE IEDM*, Dec. 2003, pp. 14.3.1–14.3.4.

[34] H. Reisinger, T. Grasser, W. Gustin, and C. Schluender, "The statistical analysis of individual defects constituting NBTI and its implications for modeling DC- and AC-stress," in *Proc. IEEE Int. Rel. Phys. Symp.*, May 2010, pp. 7–15.

Author's photograph and biography are not available at the time of publication.